

## Application of Anomalous Small-Angle X-Ray Scattering to Spherical Polyelectrolyte Brushes

Q. de Robillard, X. Guo, N. Dingenouts, M. Ballauff\*

Polymer-Institut, Universität Karlsruhe, Kaiserstrasse 12, 76128 Karlsruhe, Germany

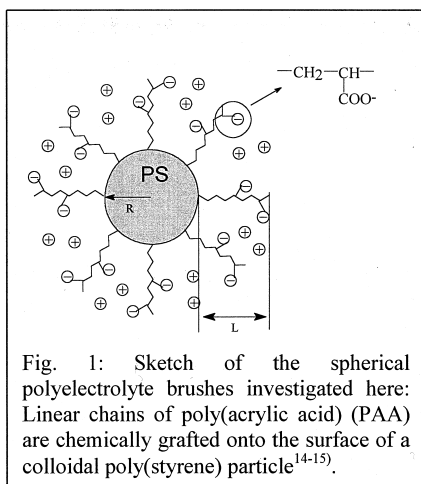
G. Goerigk

Institut für Festkörperforschung, Forschungszentrum Jülich, Postfach 1913, 52425

Jülich, Germany

**SUMMARY:** The analysis of spherical polyelectrolyte brushes by anomalous small-angle X-ray scattering (ASAXS) is considered. The particles under consideration consist of a solid poly(styrene) core onto which chains of poly(acrylic acid) are grafted. If Rubidium ions are chosen as counterions, ASAXS can be applied to the study of these systems because the absorption edge of Rb (15199.6eV) can be reached by synchrotron radiation. Here we discuss the results to be obtained by the application of ASAXS to spherical polyelectrolyte brushes.

### Introduction



If polyelectrolyte chains are densely grafted to solid surfaces, polyelectrolyte brushes result which lately have attracted much attention recently<sup>1-13</sup>. Recently, we have shown that dense polyelectrolyte brushes can be generated on the surface of colloidal latex particles by photo-emulsion polymerization<sup>14,15</sup>. The synthesis of these particles (see fig. 1) proceeds through a photochemical generation of radicals on the surface of poly(styrene) (PS) core particles. These radicals start the polymerization of water-soluble monomers as e.g. acrylic acid

(AA) directly on the surface. The contour length  $L_c$  of the resulting poly(acrylic acid) (PAA) chains and their grafting density  $\sigma$  (number of chains per  $\text{nm}^2$ ) can be varied within wide limits<sup>15</sup>. The systems thus generated can be compared to brushes prepared on flat macroscopic surfaces by a grafting-from technique<sup>6-8</sup>.

Up to now, these particles have been studied mainly by dynamic light scattering<sup>15</sup> which allows to monitor their hydrodynamic radius as function of ionic strength in the limit of high dilution. Small-angle scattering, in particular small-angle X-ray scattering (SAXS)<sup>16-18</sup> is also suitable to investigate these colloids because ions with high contrast as e.g.  $\text{Rb}^+$  or  $\text{Cs}^+$  can be chosen as counterions<sup>19</sup>. SAXS, however, does not allow to distinguish between the scattering contributions of the particle and the counterions. This problem can be circumvented by use of synchrotron radiation which allows to attain the absorption edge of heavier elements as e.g.  $\text{Rb}^{20-23}$ . Measuring the scattering intensity at different energies near the absorption edge of the element under consideration allows to assess the particular contribution of the element to the scattering signal. This method termed anomalous small-angle X-ray scattering (ASAXS) should be well suited to investigate spherical polyelectrolyte brushes carrying  $\text{Rb}^+$ -counterions. The K-edge of Rubidium is located at 15199.6eV which can be reached rather conveniently by synchrotron radiation<sup>20, 23</sup>.

Here we wish to give a first account of our recent investigations of spherical polyelectrolyte brushes by ASAXS. The main emphasis lies on a comprehensive theoretical discussion of the changes of the measured scattering curves in the immediate vicinity of the absorption edge. In addition to this, preliminary experimental data are presented that corroborate the theoretical analysis given here in a qualitative manner.

## Theory and Model Calculations

*General considerations:* We consider a dilute solution of spherical polyelectrolyte brushes dispersed in water. The polyelectrolyte chains fixed on the surface are in the fully dissociated state and the negative charge of these chains is balanced by positive counterions. In the following it can be assumed in good approximation that the counterions cannot leave the brush<sup>10,15</sup>.

The macroions consist of polymers which do not exhibit anomalous scattering in the energy range given in the experiment, only the counterions are assumed to give an anomalous contribution to the measured intensity. Since the electron density of the counterions becomes a complex function<sup>20,21)</sup>, the calculation of the intensity requires special consideration. In the following the latter contribution is calculated explicitly and studied by use of model calculations.

The absolute scattering intensities  $I(q)$  following from small-angle scattering experiment is given by<sup>16)</sup>

$$I(q) = \frac{N}{V} \cdot I_o(q)S(q) \quad (1)$$

where  $N/V$  is the number of the dissolved polyelectrolyte molecules per volume.  $S(q)$  is the structure factor which takes into account the effect of intermolecular interferences. Its influence is restricted to the region of small scattering angles and will not be considered further here<sup>17,18)</sup>. The total scattering intensity of a system of non-interacting objects follows therefore from eq.(1) with  $S(q) = 1$ .

In general, the scattering intensity  $I_o(q)$  of a single particle follows as<sup>20)</sup>

$$I_o(q) = F(q)F^*(q) \quad (2)$$

We assume a spherical symmetric particles and no averaging over different orientations is needed. Therefore the scattering amplitude  $F(q)$  is a function of the magnitude  $q$  of the scattering vector  $\vec{q}$  only. It may be formulated as follows:<sup>16)</sup>

$$F(q) = 4\pi \int_0^\infty \Delta\rho(r) \frac{\sin qr}{qr} r^2 dr \quad (3)$$

Here  $\Delta\rho(r_c)$  is the radial excess electron density of the spherical polyelectrolyte brush against the surrounding medium. It includes the real excess electron density of the macroion itself and the complex electron density of its counterions. From its derivation it is evident that eq.(3) holds also true for complex excess scattering length density  $\Delta\rho(r)$  for which the scattering amplitude  $F(q)$  becomes a complex quantity itself.

As mentioned above the macroion can be described in terms of a constant real excess electron density  $\Delta\rho_{core}$ . Let  $R_c$  denote the radius of the core. Then  $\Delta\rho(r) = \Delta\rho_{core}$  for  $r \leq R_c$ . For  $r > R_c$  the excess electron density is determined by the polyelectrolyte chains and their

counterions. The excess electron density of the polyelectrolyte chains is a real quantity, of course and the calculation of its contribution to  $I_0(q)$  can be derived from eq.(2) and (3) as usual<sup>17,18)</sup>. Only the counterions require special consideration: First of all, the integration in eq.(3) must extend over all counterions belonging to one macroion. Otherwise the condition of electroneutrality would be violated. Moreover, the number of excess electrons per counterion  $\Delta f_{ion}$  becomes a complex quantity in the vicinity of the adsorption edge. As a consequence,  $\Delta\rho(r)$  will become complex for  $R > R_c$ . Its calculation will be considered in the following.

*Scattering length density of counterions:* Let  $n_{ion}(r)$  denotes the number of counterions per unit volume within distance  $r$  of the center of the brush. Then the contribution of the counterions  $\Delta\rho_{ion}(r)$  to the excess electron density of the particles is given by  $\Delta\rho(r) = n_{ion}(r) \cdot \Delta f_{ion}$  for  $r > R_c$ . For  $r \leq R_c$  it is zero, of course. Near the absorption edge the scattering length  $f_{ion}$  of a single counterion becomes an explicit function of the energy  $E$  of the incident X-rays. It may be expressed through<sup>20,21)</sup>

$$f_{ion} = f_0 + f'(E) + f''(E) \quad (4)$$

The first term  $f_0$  is the non-resonant term which is equal to the atomic number of the element. The second and the third factor are energy dependent and show strong variation only in the vicinity of the adsorption edge. The imaginary part  $f''$  is directly related to the adsorption cross section of the X-rays. Both  $f'$  and  $f''$  are connected to each other by the Kramers-Kronig relation<sup>20,21)</sup>. Both quantities can be calculated by the routine furnished by Cromer and Liberman<sup>23)</sup>. In the following we use the values tabulated by Chantler<sup>24)</sup>.

For ions immersed in a medium of scattering length density  $\rho_m$  the contrast per ion follows as

$$\Delta\rho_{ion} = \frac{f_{ion}}{V_{ion}} - \rho_m \quad (5a)$$

where  $V_{ion}$  denotes the volume of a given ion. The volume  $V_{ion}$  must be calculated from the density of the polyelectrolyte in solution. Calculated per counterion we have

$$\Delta f_{ion} = f_0 - \rho_m V_{ion} + f' + if'' \quad (5b)$$

Here it becomes obvious that  $\Delta f_{ion}$  consists of three parts: i) the classical number of excess electrons per ion  $f_0 - \rho_m V_{ion} = \Delta f_0$ ; ii) the part related to  $f'$ , i.e., to the real part of the scattering length, and iii) the part related to the absorption, i.e. to  $f''$ . Model calculation to be

discussed further below will serve for an assessment of the relative magnitude of the intensity stemming from those three contributions.

*Calculation of the scattering intensity  $I_o(q)$ :* It is expedient to separate the resonant term  $F_{res}(q)$  of the amplitude  $F(q)$  from the non-resonant term  $F_o(q)$ . Hence,

$$F_o(q) = 4\pi \int_0^{R_c} \Delta\rho_{core} \frac{\sin qr}{qr} r^2 dr + 4\pi \int_{R_c}^{\infty} \Delta\rho_{poly}(r) \frac{\sin qr}{qr} r^2 dr + \Delta f_o \cdot 4\pi \int_{R_c}^{\infty} n_{ion}(r) \frac{\sin qr}{qr} r^2 dr \quad (6)$$

For the resonant term  $F_{res}(q)$  the foregoing reasoning leads to

$$F_{res}(q) = (f' + if'') 4\pi \int_{R_c}^{\infty} n_{ion}(r) \frac{\sin qr}{qr} r^2 dr = f' v(q) + if'' v(q) \quad (7)$$

From eq.(2) we thus obtain for the scattering intensity of a single particle

$$I_o(q) = [F_o(q) + F_{res}(q)][F_o(q) + F_{res}^*] = F_o^2(q) + 2f' F_o(q)v(q) + (f'^2 + f''^2)v^2(q) \quad (8)$$

Here the first term denotes the scattering intensity far apart from the adsorption edge. Measuring at two energies of the incident radiation this term may be removed from the

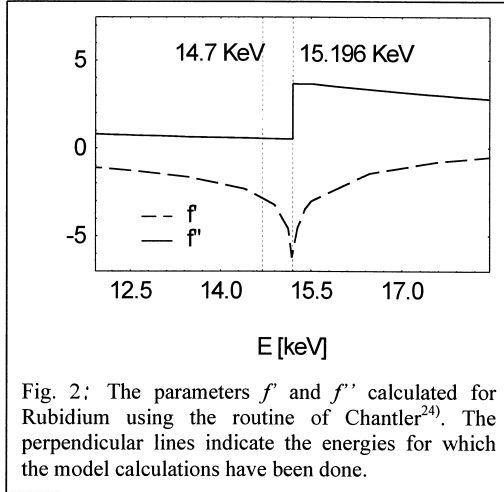


Fig. 2: The parameters  $f'$  and  $f''$  calculated for Rubidium using the routine of Chantler<sup>24</sup>. The perpendicular lines indicate the energies for which the model calculations have been done.

experimental data. The second term often represents the leading contribution to the anomalous scattering. The third term is often much smaller but becomes the leading term near the match point of the particle, i.e., when the non-resonant contrast  $\Delta f_0$  tends to zero. Then  $F_o(q)$  is small and the first two terms virtually vanish. The coefficients  $f'$  and  $f''$  are independent of contrast, of course, and the third term may become important

under these conditions. Therefore its magnitude must be checked in each case. Fig. 2 displays  $f'$  and  $f''$  as function of energy calculated for Rubidium. The strong variation of  $f'$  in the immediate vicinity of the absorption edge is directly visible. Because of the strong X-ray fluorescence as compared to the weak X-ray scattering, measurements are usually confined to energies below the edge. Here fig. 2 shows that  $f''$  is virtually a constant and the strong variation of the resonant terms is solely due to  $f'$ .

**Table 1**

Data used for model calculations

E (keV)	$f'$	$f''$
14.700	-2.85	.5546
15.196	-5.98	.5282
contrast of core $\Delta\rho_{core} = 6e^-/\text{nm}^3$		
contrast of polyelectrolyte chains in shell: $\Delta\rho_{poly} = 16e^-/\text{nm}^3$		
number of excess electrons per $\text{Rb}^+$ -ion: $\Delta f_{ion} = 31.5$		
(calculated from the Pauling radius of the $\text{Rb}^+$ -ion: 0.148nm)		

*Model calculations:*

The magnitude of the different terms can be easily assessed when looking at the result of model calculations. Here we consider a concentric core-shell particle. Table 1 gathers the parameters used in the course of these calculations.

Fig. 3a,b displays the calculated scattering intensities. Here the various contributions to the intensity are plotted against  $q$ . Fig. 3a displays the result for 14.700eV, that is markedly below the absorption edge. Here the intensity  $I_0(q)$  coincides practically with the non-resonant term  $F_0^2(q)$  of eq.(8). For the sake of clarity only  $I_0(q)$  is shown in fig. 3a. The model calculation furthermore shows that the cross term (second term of eq.(8)) is negative. Its contribution is small but measurable if precise data are available. The self term (third term of eq.(8)) is very small and may be neglected in this case. Hence, there is an appreciable difference between the intensity measured at much higher energies ( $F_0^2(q)$ , see eq. (8)) and the intensity taken in the vicinity of the absorption edge ( $I_0(q)$ , see eq.(8)). The intensity is predicted to be lowered because the cross term of  $F_0(q)$  and  $v(q)$  of eq.(8) is negative. The shift of the scattering curves is expected to be in the measurable range if absolute intensities can be obtained with good precision.

Very near to the edge, however,  $I_0(q)$  and  $F_0^2(q)$  of eq.(8) differ markedly (Fig. 3b). The calculated intensity is considerably smaller than  $F_0^2(q)$  because the negative cross term is now

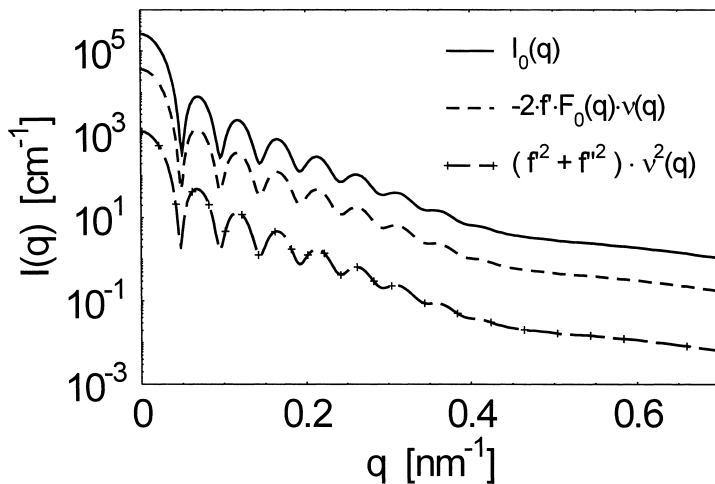


Fig. 3a

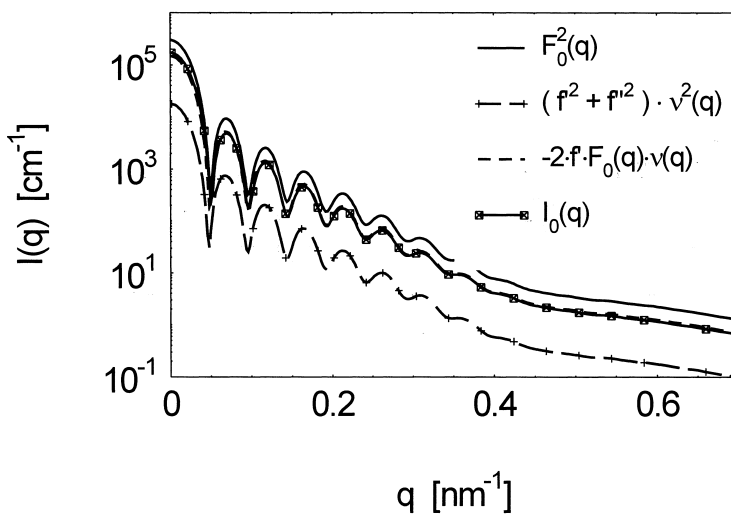


Fig. 3b

Scattering intensities calculated according to eq.(8) for core-shell particles with  $\text{Rb}^+$ -ions in the shell. The diameter of the core is 58nm, the thickness of the shell was assumed to be 15nm. The polydispersity was set to 5.2%. The curves display the various contributions according to eq.(8). Fig. 3a refers to an energy of 14.700eV whereas fig. 3b gives the calculation done for 15.196eV.

of the order of 10% of the non-resonant term  $F_0^2(q)$ . As a consequence of this, the effect of anomalous dispersion should be easily measurable. It should be noted, however, that the self-term has become much larger, too. The negative contribution of the cross-term is therefore partially canceled by this term. This effect diminishes the effect of anomalous dispersion. It is hence evident that the self-term cannot be neglected if discussing ASAXS-data of these systems in the immediate vicinity of the absorption edge.

Fig. 2 calls attention on a further important point. The imaginary part  $f''$  does not change very much with energy and its contribution to the self-term in eq.(8) stays practically constant. If the anomalous contribution is determined by subtracting scattering curves measured at different intensities this contribution will cancel out in excellent approximation. For the present system it therefore suffices to consider only contributions related to  $f'$ , i.e. the term  $f'^2 v^2(q)$  of eq. (8).

## Comparison with Experimental Data

In the following we compare the present predictions to preliminary ASAXS-data. Details of the measurements and their evaluation will be reported elsewhere. All measurements reported here are done at the JUSIFA-beamline, HASYLAB, DESY, Hamburg. The K-edge of the Rubidium ions was determined by measurements of RbCl-solutions.

Solutions of the spherical polyelectrolyte brushes (fig. 1) have been titrated up to a pH of 7 as discussed in ref.<sup>15)</sup>. Under these conditions all protons in the brush have been replaced by  $\text{Rb}^+$ -ions. No further salt was added. The solutions have been confined in capillaries of 2mm diameter. All data have been normalized to the primary intensity and have been carefully corrected for transmission, dark current, background scattering and detector sensitivity. The scattering data discussed here have been circularly averaged by using the software available at the beamline<sup>22)</sup> and have been calibrated into absolute units [ $\text{e.u./nm}^3$ ]. The positional resolution of the JUSIFA MWPC-detector is too small to resolve the minima and maxima of the scattering curves shown in fig. 3. The spherical particles are too big and the measured intensities shown in fig. 4 exhibit only the strong decay with increasing  $q$  typical for large colloidal objects.



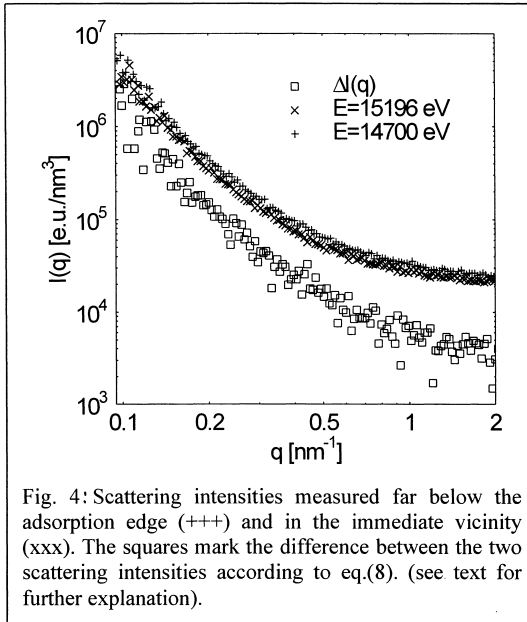


Fig. 4 demonstrates the measured scattering intensity is lowered indeed when approaching the absorption edge. It displays the scattering intensities calibrated into absolute units measured at two energies below and in the vicinity of the adsorption edge. The difference between these two scattering curves is shown as well and demonstrates that the effect of anomalous dispersion is of the sign and of the approximate magnitude predicted by theory: The measured intensity is lowered upon approaching the edge and the effect of the order of 10% if

measurements are taken in the immediate neighborhood of the adsorption edge. Theory demonstrates that the difference is given by  $F_0(q)v(q)$  (see eq.(8)) in excellent approximation. The  $q$ -dependence of  $F_0(q)v(q)$  largely resembles the one of  $F_0^2(q)$  which is found experimentally, too.

As mentioned above, the spherical polyelectrolyte brushes investigated here are too big so that the minima and maxima of the formfactor of spherical objects (see fig. 3) cannot be resolved. Therefore no quantitative analysis can be done along the lines given here. The preliminary data shown in figure 4, however, clearly demonstrate that ASAXS is a powerful tool when dealing with ionic systems.

### Acknowledgement

Financial support by the Deutsche Forschungsgemeinschaft, Schwerpunkt "Polyelektrolyte", is gratefully acknowledged.

## Literature

1. G. J. Fleer, M. A. Cohen Stuart, J. M. H. M. Scheutjens, T. Cosgrove, B. Vincent, *Polymers at Interfaces*; Chapman and Hall, London 1993
2. P. Pincus, *Macromolecules* **24**, 2912 (1991)
3. E. B. Zhulina, O. V. Borisov, T. M. Birshtein, *J. Phys. II (France)* **2**, 63 (1992)
4. O. V. Borisov, E. B. Zhulina, T. M. Birshtein, *Macromolecules* **27**, 4795 (1994).
5. E. B. Zhulina, T. M. Birshtein, O. V. Borisov, *Macromolecules* **28**, 1491 (1995)
6. O. Prucker, J. R  he, *Macromolecules* **31**, 592 (1998)
7. O. Prucker, J. R  he, *Macromolecules* **31**, 602 (1998)
8. O. Prucker, M. Schimmel, G. Tovar, W. Knoll, J. R  he, *Adv. Mater.* **10**, 1073 (1999)
9. C. Biver, R. Hariharan, J. Mays, W. B. Russel, *Macromolecules* **30**, 1787 (1997)
10. R. Hariharan, C. Biver, J. Mays, W. B. Russel, *Macromolecules* **31**, 7506 (1998)
11. H. Ahrens, S. F  rster, Ch. Helm, *Phys. Rev. Lett.* **81**, 4172 (1998)
12. Y. Tran, P. Auroy, L.-T. Lee, *Macromolecules* **32**, 8952 (1999)
13. Y. Tran, P. Auroy, L.-T. Lee, M. Stamm, *Phys. Rev. E* **60**, 6984 (1999)
14. X. Guo, A. Weiss, M. Ballauff, *Macromolecules* **32**, 6043 (1999)
15. X. Guo, M. Ballauff, *Langmuir*, in press
16. O. Glatter, O. Kratky, Eds. *Small Angle X-Ray Scattering*, Academic Press, London 1982
17. M. Ballauff, J. Bolze, N. Dingenouts, P. Hickl, D. P  tschke, *Macromol Chem. Phys.* **197**, 3043 (1996)
18. N. Dingenouts, J. Bolze, D. P  tschke, M. Ballauff, *Adv. Polym. Sci.* **144**, 1 (1999)
19. Q. de Robillard, X. Guo, M. Ballauff, *Macromolecules*, accepted
20. H. B. Stuhmann, *Adv. Polym. Sci.* **67**, 123 (1985)
21. H. B. Stuhmann, G. Goerigk, B. Munk, in *Handbook of Synchrotron Radiation*, Vol. 4, chapter 17, S. Ebashi, M. Koch, E. Rubenstein, eds., Elsevier
22. H.-G. Haubold, K. Gruenhagen, M. Wagener, H. Jungbluth, H. Heer, A. Pfeil, H. Rongen, G. Brandenburg, R. Moeller, J. Matzerath, P. Hiller, H. Halling, *Rev. Sci. Instr.* **60**, 1943 (1989)
23. D. T. Cromer, D. A. Liberman, *Acta Cryst.* **A37**, 267 (1981)
24. C. T. Chantler, *J. Phys. Chem. Ref. Data* **24**, 71 (1995)